Int. J. Solids Structures Vol. 26, No. 7, pp. 779–799, 1990
Printed in Great Britain.

0020–7683/90 $3.00 + .00

STIFFENED PLATES WITH ARBITRARILY OBLIQUE STIFFENERS

CHONG JIN WON
Department of Mechanics and Design, Kookmin University, Seoul, Korea

(*Received* 14 *September* 1988; *in revised form* 4 *October* 1989)

Abstract—An analysis for a stiffened plate with arbitrarily oblique and equally spaced eccentric stiffeners is proposed. In this analysis, the joint effects of stiffeners by the interaction of the plate and stiffeners are taken into account and the effects of stiffeners are not considered as discrete members, but their effects are averaged or "smeared out" over the plate. The equilibrium equations and boundary conditions are derived by applying the principle of minimum potential energy. In cases where the orthogonally and symmetrically oblique stiffened plates with simply-supported four edges are subjected to a uniform lateral load, the rigorous values of the midpoint deflection of the plate obtained by considering the joint effects are compared with those values obtained by neglecting the joint effects. For both stiffening cases, the equivalent rigidities which are used in the Huber-type equilibrium equation are determined by assuming that the gradients of the in-plane stress resultants are zero and these are compared with the values obtained by using the concept of adjusted centroids. The approximate solutions obtained by using these equivalent rigidities are compared with the rigorous values for both stiffening cases with simply-supported four edges under uniform lateral loads.

1. INTRODUCTION

The stiffened plate is a common structural form in buildings, bridges, ships and aircraft. In general, stiffened plates with conventional (orthogonal) stiffening or symmetrically oblique stiffening by closely spaced stiffeners can be regarded as an equivalent plate of uniform thickness in which the *effects of stiffeners are averaged or smeared out over the area of the plate.*

The application of classical flexural theory of elastic thin plates of homogeneous orthotropic material to the problem of orthogonally stiffened plates was first suggested by Huber (1923). He presented expressions for the flexural rigidities which are used in the orthotropic plate equations. The orthotropic plate theory based on the Huber equation has since been applied to the analysis of grid systems and orthogonally stiffened plates (Giencke, 1955; Huffington, 1956; Massonet, 1959; Cusens *et al.*, 1972; Nishino *et al.*, 1974; Hasegawa *et al.*, 1975).

In many structures like bridge decks, the stiffeners are placed on one side of the plate only. If the stiffeners are placed only on one side of the plate, the eccentricities of the stiffeners must be taken into account because of the strains in the middle surface of the plate. Hence, the calculation of the stiffness coefficients with respect to the unknown neutral surface complicates the problem. An improved theory which considers the extensibility of the middle plane of the plate which introduced additional shear stresses was first formulated by Pflüger (1947) for the treatment of buckling problems of stiffened plates. The governing differential equations are expressed in terms of the in-plane as well as transverse displacement components of the middle surface of the plate. This theory has been applied to the stiffened plate problems by many investigators (Trensk, 1954; Giencke, 1955; Clifton *et al.*, 1956; Massonet, 1959; McElman *et al.*, 1966; Srinivasan and Thiruvenkatachari, 1985).

Most of above investigations have been treated by neglecting the joint effects of stiffeners in the orthogonal stiffening case and only a few authors have considered them on the equivalent rigidities in the orthogonal stiffening case (Cusens *et al.*, 1972; Nishino *et al.*, 1974; Hasegawa *et al.*, 1975). For the symmetrically oblique stiffening case, a few papers are available (Dow *et al.*, 1954; Meyer, 1967; Karmakar, 1979) and to the author's knowledge, there is no literature on a stiffened plate with arbitrarily oblique stiffeners in which the joint effects of the stiffeners are considered.

In this study, a stiffened plate with arbitrarily oblique and equally spaced eccentric stiffeners is treated. In formulating the potential energy of the system, the stiffness coefficients are obtained by smearing out the effects of the stiffeners under the assumption that the plate and stiffeners behave as a monolithic structure. The equilibrium equations in which the eccentricity and the joint effects of the stiffeners are taken into account are derived by applying the principle of minimum potential energy.

The closed-form solutions of the midpoint deflections for the orthogonally and symmetrically oblique stiffened, rectangular plates with simply-supported edges subjected to a uniform lateral load are obtained and the midpoint deflections obtained by including the joint effects are compared with those values obtained by neglecting the joint effects.

The equivalent rigidities of the stiffened plate are determined by assuming that the gradients of the in-plane stress resultants are zero and these values are compared with those values obtained by different means, namely, by using the concept of adjusted centroids. For both stiffening cases, the approximate solutions which are obtained by using these equivalent rigidities are compared with the closed-form solutions.

2. DERIVATION OF EQUATIONS

Figure 1 shows the configuration of the stiffened plate with arbitrarily oblique and equally spaced eccentric stiffeners and Fig. 2 shows a typical element of the oblique stiffeners with rectangular cross-sections. In analyzing deformations of the infinitesimal element, the following are assumed in addition to the basic assumptions which are used in linear plate theory.

(a) The stiffeners are closely and equally spaced on one side of the plate with arbitrary angles.

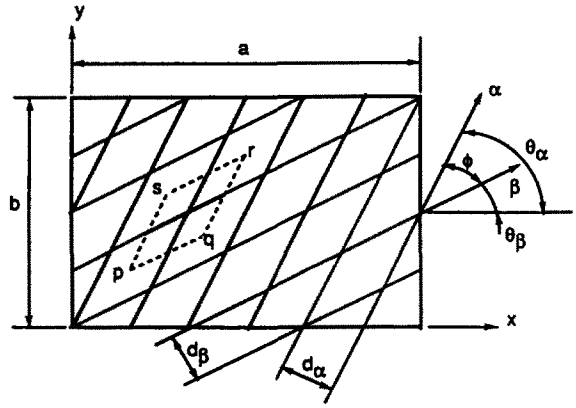

Fig. 1. Rectangular plate with equally spaced and arbitrarily oblique eccentric stiffeners.

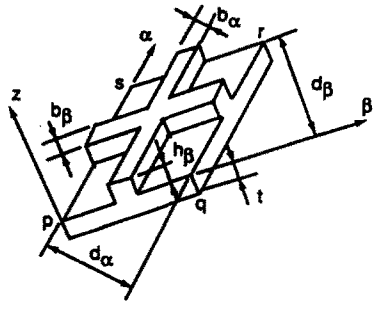

Fig. 2. Detail of the skew element, indicated in Fig. 1.

(b) The state of stress of the stiffeners is biaxial at the joints of two intersecting stiffeners and uniaxial elsewhere.

(c) The plate and stiffeners act as a monolithic element for shear deformation and the continuity condition is satisfied in the contact areas between the plate and the intersection parts of the stiffeners.

Strain–displacement relations

In orthogonal Cartesian coordinates, the strains ε_x, ε_y and γ_{xy} in a plate at a distance z from the middle plane of the plate can be written as

$$\begin{aligned} \varepsilon_x &= \varepsilon_x^0 - zw_{,xx} \\ \varepsilon_y &= \varepsilon_y^0 - zw_{,yy} \\ \gamma_{xy} &= \gamma_{xy}^0 - 2zw_{,xy} \end{aligned} \tag{1}$$

where strains ε_x^0, ε_y^0 and γ_{xy}^0 in the middle plane of the plate are represented by the displacements u, v and w as follows:

$$\begin{aligned} \varepsilon_x^0 &= u_{,x} \\ \varepsilon_y^0 &= v_{,y} \\ \gamma_{xy}^0 &= u_{,y} + v_{,x}. \end{aligned} \tag{2}$$

The strains ε_α, ε_β and $\gamma_{\alpha\beta}$ in the plate at a distance z from the middle plane of the plate are expressed in oblique coordinates as shown in Fig. 1:

$$\begin{aligned} \varepsilon_\alpha &= \varepsilon_\alpha^0 - zw_{,\alpha\alpha} \\ \varepsilon_\beta &= \varepsilon_\beta^0 - zw_{,\beta\beta} \\ \gamma_{\alpha\beta} &= \gamma_{\alpha\beta}^0 - 2zw_{,\alpha\beta} \end{aligned} \tag{3}$$

where

$$\begin{Bmatrix} \varepsilon_\alpha^0 \\ \varepsilon_\beta^0 \\ \gamma_{\alpha\beta}^0 \end{Bmatrix} = \begin{bmatrix} \cos^2\theta_\alpha & \sin^2\theta_\alpha & \sin\theta_\alpha\cos\theta_\alpha \\ \cos^2\theta_\beta & \sin^2\theta_\beta & \sin\theta_\beta\cos\theta_\beta \\ 2\cos\theta_\alpha\cos\theta_\beta & 2\sin\theta_\alpha\sin\theta_\beta & \sin(\theta_\alpha+\theta_\beta) \end{bmatrix} \begin{Bmatrix} \varepsilon_x^0 \\ \varepsilon_y^0 \\ \gamma_{xy}^0 \end{Bmatrix} \tag{4}$$

and

$$\begin{Bmatrix} w_{,\alpha\alpha} \\ w_{,\beta\beta} \\ w_{,\alpha\beta} \end{Bmatrix} = \begin{bmatrix} \cos^2\theta_\alpha & \sin^2\theta_\alpha & \sin 2\theta_\alpha \\ \cos^2\theta_\beta & \sin^2\theta_\beta & \sin 2\theta_\beta \\ \cos\theta_\alpha\cos\theta_\beta & \sin\theta_\alpha\sin\theta_\beta & \sin(\theta_\alpha+\theta_\beta) \end{bmatrix} \begin{bmatrix} w_{,xx} \\ w_{,yy} \\ w_{,xy} \end{bmatrix}. \tag{5}$$

Stress–strain relations

The stress–strain relations for the plate are expressed in orthogonal Cartesian coordinates:

$$\begin{aligned} \sigma_x &= \frac{E}{1-\nu^2}(\varepsilon_x + \nu\varepsilon_y) \\ \sigma_y &= \frac{E}{1-\nu^2}(\varepsilon_y + \nu\varepsilon_x). \end{aligned} \tag{6}$$

In oblique coordinates, the stress–strain relations are expressd as (see, e.g., Argiris, 1966):

$$\begin{Bmatrix} \varepsilon_\alpha \\ \varepsilon_\beta \\ \gamma_{\alpha\beta} \end{Bmatrix} = \frac{1}{E}\begin{bmatrix} A_{11} & A_{12} & A_{13} \\ A_{21} & A_{22} & A_{23} \\ A_{31} & A_{32} & A_{33} \end{bmatrix}\begin{Bmatrix} \sigma_\alpha \\ \sigma_\beta \\ \tau_{\alpha\beta} \end{Bmatrix} \tag{7}$$

where

$$\begin{aligned} A_{11} &= 1 \\ A_{12} &= A_{21} = \cos^2\phi - \nu\sin^2\phi \\ A_{13} &= A_{31} = 2\cos\phi \\ A_{22} &= 1 \\ A_{23} &= A_{32} = A_{13} \\ A_{33} &= 2(1+\nu)\sin^2\phi + 4\cos^2\phi. \end{aligned} \tag{8}$$

From assumption (b), if the stiffeners are subjected to axial forces resulting in uniformly distributed stresses σ_α and σ_β, the strains ε_α and ε_β, which are averaged over the stiffener lengths, can be given by

$$\begin{aligned} \varepsilon_\alpha &= \frac{1}{E}[\sigma_\alpha(1-\eta_\beta) + (A_{11}\sigma_\alpha + A_{12}\sigma_\beta + A_{13}\tau_{\alpha\beta})\eta_\beta] \\ \varepsilon_\beta &= \frac{1}{E}[\sigma_\beta(1-\eta_\alpha) + (A_{21}\sigma_\alpha + A_{22}\sigma_\beta + A_{23}\tau_{\alpha\beta})\eta_\alpha] \end{aligned} \tag{9}$$

where

$$\begin{aligned} \eta_\alpha &= \frac{b_\alpha}{d_\alpha} \\ \eta_\beta &= \frac{b_\beta}{d_\beta}. \end{aligned} \tag{10}$$

From eqns (7) and (9), σ_α and σ_β can be expressed as:

$$\begin{aligned} \sigma_\alpha &= E(A_1\varepsilon_\alpha + A_2\varepsilon_\beta + A_3\gamma_{\alpha\beta}) \\ \sigma_\beta &= E(B_1\varepsilon_\alpha + B_2\varepsilon_\beta + B_3\gamma_{\alpha\beta}) \end{aligned} \tag{11}$$

where

$$A_1 = \frac{1 - \dfrac{A_{13}^2}{A_{33}}\eta_\alpha}{\lambda}$$

$$A_2 = \frac{-\left(A_{12} - \dfrac{A_{13}^2}{A_{33}}\right)\eta_\beta}{\lambda}$$

$$A_3 = \frac{\left(A_{12} - \frac{A_{13}^2}{A_{33}}\right)\frac{A_{13}}{A_{33}}\eta_\alpha\eta_\beta - \left(1 - \frac{A_{13}^2}{A_{33}}\eta_\alpha\right)\frac{A_{13}}{A_{33}}\eta_\beta}{\lambda}$$

$$B_1 = \frac{-\left(A_{12} - \frac{A_{13}^2}{A_{33}}\right)\eta_\alpha}{\lambda}$$

$$B_2 = \frac{1 - \frac{A_{13}^2}{A_{33}}\eta_\beta}{\lambda}$$

$$B_3 = \frac{\left(A_{12} - \frac{A_{13}^2}{A_{33}}\right)\frac{A_{13}}{A_{33}}\eta_\alpha\eta_\beta - \left(1 - \frac{A_{13}^2}{A_{33}}\eta_\beta\right)\frac{A_{13}}{A_{33}}\eta_\alpha}{\lambda}$$

$$\lambda = \left(1 - \frac{A_{13}^2}{A_{33}}\eta_\beta\right)\left(1 - \frac{A_{13}^2}{A_{33}}\eta_\alpha\right) - \left(A_{12} - \frac{A_{13}^2}{A_{33}}\right)^2\eta_\alpha\eta_\beta. \tag{12}$$

From assumption (c), if the stiffeners resist the horizontal shear forces, the shear stress of the grid system on the horizontal section $\bar{\tau}_{xy}$ can be expressed by:

$$\bar{\tau}_{xy} = \xi G\bar{\gamma}_{xy} \tag{13}$$

where

$$\bar{\gamma}_{xy} = (\gamma_{xy}^0 - 2zw_{,xy})$$

$$\xi = \frac{\eta_\alpha\eta_\beta}{\eta_\alpha + \eta_\beta}. \tag{14}$$

The shear forces of the grid system can be assumed to be transmitted through the normal stresses in the stiffeners since the shear stresses may be carried by the plate alone when the stiffeners are connected with a coherent plate (see, e.g., Flügge, 1973) and from eqn (13), the normal stresses $\bar{\sigma}_\alpha$ and $\bar{\sigma}_\beta$ in the oblique stiffeners can be given by (Morley, 1963):

$$\bar{\sigma}_\alpha = -\xi G \operatorname{cosec}\phi \sin 2\theta_\beta\bar{\gamma}_{xy}$$

$$\bar{\sigma}_\beta = -\xi G \operatorname{cosec}\phi \sin 2\theta_\alpha\bar{\gamma}_{xy}. \tag{15}$$

Energy expressions

If the displacements in the plate and stiffeners are continuous and the effects of the stiffeners are averaged over the plate, from eqns (11) and (15), the strain energy of the oblique stiffeners U_{st} in which the joint effects of stiffeners are considered can be taken as

$$U_{st} = \frac{1}{2}\int_0^a\int_0^b \left\{\frac{1}{d_\alpha}\int_{A_\alpha}(\sigma_\alpha + \bar{\sigma}_\alpha)\varepsilon_\alpha \,\mathrm{d}A_\alpha + \frac{1}{d_\beta}\int_{A_\beta}(\sigma_\beta + \bar{\sigma}_\beta)\varepsilon_\beta \,\mathrm{d}A_\beta + G\left[\frac{J_\alpha}{d_\alpha}(w_{,\alpha\alpha})^2 + \frac{J_\beta}{d_\beta}(w_{,\beta\beta})^2\right]\right\}\mathrm{d}x\,\mathrm{d}y \tag{16}$$

where A_α and A_β are the cross-sectional areas of the stiffeners in the α and β directions, respectively, and J_α and J_β are their torsional constants, which are given in the Apppendix. The strain energy of the unstiffened plate U_p is represented as

$$U_p = \frac{C}{2}\int_0^a\int_0^b \left[(\varepsilon_x^0)^2 + 2\nu\varepsilon_x^0\varepsilon_y^0 + (\varepsilon_y^0)^2 + \frac{(1-\nu)}{2}(\gamma_{xy}^0)^2\right] dx\,dy$$

$$+ \frac{D}{2}\int_0^a\int_0^2 \left[w_{,xx}^2 + 2\nu w_{,xx}w_{,yy} + w_{,yy}^2 + \frac{(1-\nu)}{2}w_{,xy}^2\right] dx\,dy \quad (17)$$

where

$$C = \frac{Et}{(1-\nu^2)}$$

$$D = \frac{Et^3}{12(1-\nu^2)}. \quad (18)$$

The potential energy V_q of the external lateral load q is represented as

$$V_q = q\int_0^a\int_0^b w\,dx\,dy. \quad (19)$$

The total energy of the stiffened plate, Π, can be expressed as

$$\Pi = U_p + U_{st} + V_q. \quad (20)$$

Substituting eqns (1), (3), (4) and (5) into eqn (16) and then from eqns (16), (17), (19) and (20), Π can be expressed as follows:

$$\Pi = \frac{1}{2}\int_0^a\int_0^b \{\varepsilon\}^t[C]\{\varepsilon\}\,dx\,dy - q\int_0^a\int_0^b w\,dx\,dy \quad (21)$$

in which

$$\{\varepsilon\} = \{\varepsilon_x^0, \varepsilon_y^0, \gamma_{xy}^0, -w_{,xx}, -w_{,yy}, -w_{,xy}\}^t \quad (22)$$

and the coefficients C_{ij} of the stiffness matrix $[C]$ are given in the Appendix. The C_{ij} are the same as those obtained by Brush and Almroth (1975) for the orthogonal stiffening case ($\theta_\alpha = 90°$, $\theta_\beta = 0°$ or $\theta_\alpha = 0°$, $\theta_\beta = -90°$) and C_{ij} for the symmetrically oblique stiffening case ($\theta_\alpha = -\theta_\beta = \theta_s$), in which the joint effects are not considered, are the same as those obtained by Karmakar (1979).

Equilibrium equations and associated boundary conditions

By substituting eqn (2) into eqn (21) and then taking the first variation of eqn (21) with respect to the displacements u, v and w, we obtain the three equilibrium equations for the stiffened plate with arbitrarily oblique stiffeners:

$$[C_{11}u_{,x} + C_{12}v_{,y} + C_{13}(u_{,y} + v_{,x}) - C_{14}w_{,xx} - C_{15}w_{,yy} - C_{16}w_{,xy}]_{,x}$$
$$+ [C_{31}u_{,x} + C_{32}v_{,y} + C_{33}(u_{,y} + v_{,x}) - C_{34}w_{,xx} - C_{35}w_{,yy} - C_{36}w_{,xy}]_{,y} = 0$$
$$[C_{21}u_{,x} + C_{22}v_{,y} + C_{23}(u_{,y} + v_{,x}) - C_{24}w_{,xx} - C_{25}w_{,yy} - C_{26}w_{,xy}]_{,y}$$
$$+ [C_{31}u_{,x} + C_{32}v_{,y} + C_{33}(u_{,y} + v_{,x}) - C_{34}w_{,xx} - C_{35}w_{,yy} - C_{36}w_{,xy}]_{,x} = 0$$
$$[C_{41}u_{,x} + C_{42}v_{,y} + C_{43}(u_{,y} + v_{,x}) - C_{44}w_{,xx} - C_{45}w_{,yy} - C_{46}w_{,xy}]_{,xx}$$
$$+ [C_{61}u_{,x} + C_{62}v_{,y} + C_{63}(u_{,y} + v_{,x}) - C_{64}w_{,xx} - C_{65}w_{,yy} - C_{66}w_{,xy}]_{,xy}$$
$$+ [C_{51}u_{,x} + C_{52}v_{,y} + C_{53}(u_{,y} + v_{,x}) - C_{54}w_{,xx} - C_{55}w_{,yy} - C_{56}w_{,xy}]_{,yy} = -q. \quad (23)$$

The boundary conditions are given in the Appendix.

3. SOLUTIONS OF ORTHOTROPIC PLATES

From eqn (23), equilibrium equations which can be used for orthogonal stiffening and symmetrically oblique stiffening with the orthotropic behavior are obtained as follows:

$$
\begin{aligned}
&[C_{11}u_{,x}+C_{12}v_{,y}-C_{14}w_{,xx}-C_{15}w_{,yy}]_{,x}+[C_{33}(u_{,y}+v_{,x})-C_{36}w_{,xy}]_{,y}=0\\
&[C_{21}u_{,x}+C_{22}v_{,y}-C_{24}w_{,xx}-C_{25}w_{,yy}]_{,y}+[C_{33}(u_{,y}+v_{,x})-C_{36}w_{,xy}]_{,x}=0\\
&[C_{41}u_{,x}+C_{42}v_{,y}-C_{44}w_{,xx}-C_{45}w_{,yy}]_{,xx}+[C_{63}(u_{,y}+v_{,x})-C_{66}w_{,xy}]_{,xy}\\
&\qquad+[C_{51}u_{,x}+C_{52}v_{,y}-C_{54}w_{,xx}-C_{55}w_{,yy}]_{,yy}=-q. \qquad (24)
\end{aligned}
$$

The closed-form and approximate solutions of the governing differential equation for orthotropic plates under various natural and geometric boundary conditions have been presented by several investigators (Trenks, 1954; Clifton *et al.*, 1956). Herein, the double series solutions and approximate solutions by the Huber-type equation (Huber, 1923) for the case of a simply-supported rectangular orthotropic plate under the lateral load are examined.

Closed-form solution

The displacement functions u, v and w for the simply-supported boundary condition can be assumed as follows:

$$
\begin{aligned}
u &= \sum_{m=1}^{\infty}\sum_{n=1}^{\infty} U_{mn}\,\mathrm{cps}\,\frac{m\pi x}{a}\sin\frac{n\pi y}{b}\\
v &= \sum_{m=1}^{\infty}\sum_{n=1}^{\infty} V_{mn}\sin\frac{m\pi x}{a}\cos\frac{n\pi y}{b}\\
w &= \sum_{m=1}^{\infty}\sum_{n=1}^{\infty} W_{mn}\sin\frac{m\pi x}{a}\sin\frac{n\pi y}{b} \qquad (25)
\end{aligned}
$$

in which U_{mn}, V_{mn} and W_{mn} are constants. The load q can be represented as a double sine series

$$
q=\sum_{m=1}^{\infty}\sum_{n=1}^{\infty} Q_{mn}\sin\frac{m\pi x}{a}\sin\frac{n\pi y}{b} \qquad (26)
$$

in which the coefficients Q_{mn} is given by

$$
Q_{mn}=\frac{4}{ab}\int_0^a\int_0^b q(x,y)\sin\frac{m\pi x}{a}\sin\frac{n\pi x}{b}\,\mathrm{d}x\,\mathrm{d}y. \qquad (27)
$$

In eqn (27), Q_{mn} for the uniformly distributed lateral load $\bar{q}$ is given as

$$
Q_{mn}=\frac{16\bar{q}}{\pi^2 mn}\quad (m,n=1,3,\ldots). \qquad (28)
$$

Substituting eqns (25) and (26) into eqn (24), a set of three linear equations in the three unknowns U_{mn}, V_{mn} and W_{mn} can be obtained for each combination of m and n. This linear system can be put into the following form:

$$
\begin{bmatrix} B_{11} & B_{12} & B_{13}\\ B_{21} & B_{22} & B_{23}\\ B_{31} & B_{32} & B_{33}\end{bmatrix}\begin{bmatrix} U_{mn}\\ V_{mn}\\ W_{mn}\end{bmatrix}=\begin{bmatrix} 0\\ 0\\ \dfrac{Q_{mn}}{E}\end{bmatrix} \qquad (29)
$$

and the elements of the matrix $[B]$ are given by

$$
\begin{aligned}
B_{11} &= C_{11}\bar{m}^2+C_{33}\bar{n}^2\\
B_{12} &= (C_{12}+C_{33})\bar{m}\bar{n}\\
B_{13} &= -C_{14}\bar{m}^3-(C_{15}+C_{36})\bar{m}\bar{n}^2\\
B_{21} &= B_{12}\\
B_{22} &= C_{33}\bar{m}^2+C_{22}\bar{n}^2\\
B_{23} &= -C_{25}\bar{n}^3-(C_{15}+C_{36})\bar{m}^2\bar{n}\\
B_{31} &= B_{13}\\
B_{32} &= B_{23}\\
B_{33} &= C_{44}\bar{m}^4+(2C_{45}+C_{66})\bar{m}^2\bar{n}^2+C_{55}\bar{n}^4
\end{aligned}
\tag{30}
$$

where $\bar{m} = m\pi/a$ and $\bar{n} = n\pi/b$. The complete solution is obtained by substituting the values U_{mn}, V_{mn} and W_{mn} obtained from eqn (29) into eqn (25).

Approximate solution by a Huber-type equation

Several approximate theories have been developed by introducing additional assumptions so that the governing differential equations may be simplified. Most of these approximate theories lead to a Huber-type equation as follows:

$$D_x w_{,xxxx}+2Hw_{,xxyy}+D_y w_{,yyyy} = q \tag{31}$$

where the constants D_x and D_y represent the bending rigidities in the x and y directions. The constant H is computed from the torsional rigidity and Poisson's ratio of the plate.

One of the widely accepted approximate methods for determining the equivalent rigidities is to assume that the normal strain is zero at the adjusted centroid of the cross section in each direction (Giencke, 1955). Another method is to use the assumption that the gradients of the in-plane stress resultants are zero (Hasegawa *et al.*, 1975). From eqn (24), the equivalent rigidities by the latter method are obtained as the following. The three equilibrium equations for the bending of the thin plate which are represented with the stress resultants can be given by

$$N_{x,x}+N_{xy,y} = 0 \tag{32a}$$

$$N_{xy,x}+N_{y,y} = 0 \tag{32b}$$

$$M_{x,xx}+2M_{xy,xy}+M_{y,yy} = -q \tag{32c}$$

where

$$N_x = C_{11}u_{,x}+C_{12}v_{,y}-C_{14}w_{,xx}-C_{15}w_{,yy} \tag{33a}$$

$$N_y = C_{21}u_{,x}+C_{22}v_{,y}-C_{24}w_{,xx}-C_{25}w_{,yy} \tag{33b}$$

$$N_{xy} = C_{33}(u_{,y}+v_{,x})-C_{36}w_{,xy} \tag{33c}$$

$$M_x = C_{41}u_{,x}+C_{42}v_{,y}-C_{44}w_{,xx}-C_{45}w_{,yy} \tag{33d}$$

$$M_y = C_{51}u_{,x}+C_{52}v_{,y}-C_{54}w_{,xx}-C_{55}w_{,yy} \tag{33e}$$

$$M_{xy} = [C_{63}(u_{,y}+v_{,x})-C_{66}w_{,xy}]/2. \tag{33f}$$

From eqns (33a, b, c), $u_{,x}$, $v_{,y}$ and $(u_{,y}+v_{,x})$ can be given by

$$\begin{aligned} u_{,x} &= e'_x w_{,xx} - e_{yx} w_{,yy} + C_1 N_x - C_3 N_y \\ v_{,y} &= e'_y w_{,yy} - e_{xy} w_{,xx} + C_2 N_y - C_3 N_x \\ u_{,y}+v_{,x} &= \frac{C_{36}}{C_{33}} w_{,xy} + \frac{N_{xy}}{C_{33}} \end{aligned} \tag{34}$$

where

$$\begin{aligned} e'_x &= \frac{C_{14}C_{22}-C_{12}C_{24}}{C_{11}C_{22}-C_{12}^2} \\ e'_y &= \frac{C_{25}C_{11}-C_{12}C_{15}}{C_{11}C_{22}-C_{12}^2} \\ e_{xy} &= \frac{C_{12}C_{14}-C_{24}C_{11}}{C_{11}C_{22}-C_{12}^2} \\ e_{yx} &= \frac{C_{12}C_{25}-C_{15}C_{22}}{C_{11}C_{22}-C_{12}^2} \\ C_1 &= \frac{C_{22}}{C_{11}C_{22}-C_{12}^2} \\ C_2 &= \frac{C_{11}}{C_{11}C_{22}-C_{12}^2} \\ C_3 &= \frac{C_{12}}{C_{11}C_{22}-C_{12}^2}. \end{aligned} \tag{35}$$

Substituting eqn (34) into eqns (33d, e, f), from eqns (33d, e, f) and (32c), the following is obtained:

$$D_x w_{,xxxx} + 2H w_{,xxyy} + D_y w_{,yyyy} = q + D_a N_{x,xx} + D_b N_{y,xx} + D_c N_{x,yy} + D_d N_{y,yy} \tag{36}$$

where

$$\begin{aligned} D_x &= C_{44} + C_{42} e_{xy} - C_{41} e'_x \\ D_y &= C_{55} + C_{51} e_{yx} - C_{52} e'_y \\ 2H &= 2D_{xy} + D_1 + D_2 \\ D_{xy} &= \left(C_{66} - \frac{C_{36}^2}{C_{33}}\right)\Big/ 2 \\ D_1 &= C_{45} + C_{41} e_{yx} - C_{42} e'_y \\ D_2 &= C_{54} + C_{52} e_{xy} - C_{51} e'_x \\ D_a &= C_{41} C_1 - C_{42} C_3 - \frac{C_{36}}{C_{33}} \\ D_b &= C_{42} C_2 - C_{41} C_3 \\ D_c &= C_{51} C_1 - C_{52} C_3 \\ D_d &= C_{52} C_1 - C_{51} C_3 - \frac{C_{36}}{C_{33}}. \end{aligned} \tag{37}$$

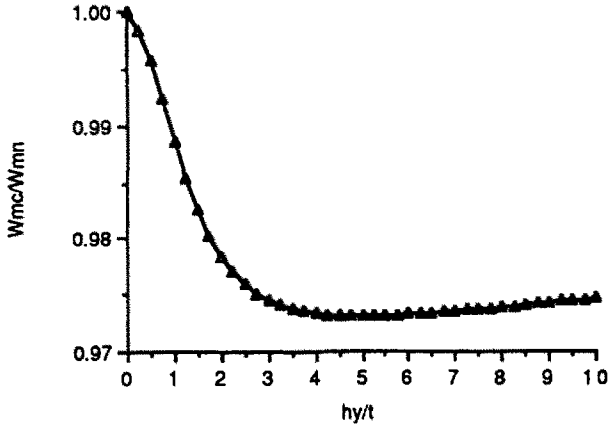

Fig. 3. Joint effects on closed-form solutions of the midpoint deflection for the orthogonally stiffened, rectangular plate with simply-supported edges under the uniform lateral load ($b_x = b_y = t$, $h_x = h_y$, $d_x = d_y = 10t$). The curve shows the midpoint deflection w_{mc} where the joint effects of the stiffeners are taken into account normalized by the value w_{mn} where the joint effects are neglected for the stiffener height h_y/t.

By assuming that the gradients of the stress resultants are zero, eqn (36) can be used as the Huber-type equation.

The equivalent rigidities obtained by Giencke (1955) are given in the Appendix.

In the case of a simply-supported rectangular orthotropic plate under a lateral load $q(x, y)$, the displacement w is represented as

$$w = \frac{4}{ab}\sum_{m=1}^{\infty}\sum_{n=1}^{\infty}\int_0^b\int_0^a\left[\frac{q(x,y)\sin(\bar{m}x)\sin(\bar{n}y)}{(\bar{m}^4)D_x+2H(\bar{m}^2\bar{n}^2)+(\bar{n}^4)D_y}\right]dx\,dy\cdot\sin(\bar{m}x)\sin(\bar{n}y). \tag{38}$$

In the case of a uniformly distributed load $\bar{q}$, from eqns (26), (27) and (38), w is written as

$$w = \frac{16\bar{q}}{\pi^6}\sum_{m=1}^{\infty}\sum_{n=1}^{\infty}\frac{\sin(\bar{m}x)\sin(\bar{n}y)}{(\bar{m}^4)D_x+2H(\bar{m}^2\bar{n}^2)+(\bar{n}^4)D_y} \tag{39}$$

4. NUMERICAL RESULTS AND DISCUSSION

Numerical results are obtained in order to study the joint effects of stiffeners for the orthogonal and symmetrically oblique stiffening cases. In all cases, the stiffeners have rectangular cross-sections and the breadths of the stiffeners and the spacing between stiffeners are constant (i.e. $b_x = b_y = t$, $d_x = d_y = 10t$ for the orthogonal stiffening case, $b_\alpha = b_\beta(= b_s) = t$, $d_\alpha = d_\beta(= d_s) = 10t$ for the symmetrically oblique stiffening case). The equivalent bending and torsional rigidities are obtained by two methods, i.e. one by using the concept of adjusted centroids (method A) and the other by assuming that the gradients of the in-plane stress resultants are zero (method B).

Joint effects on the closed-form solution

Figures 3 and 4 show the ratios of the midpoint deflection of the plate obtained rigorously by considering the joint effects (w_{mc}) to those obtained by neglecting them (w_{mn})

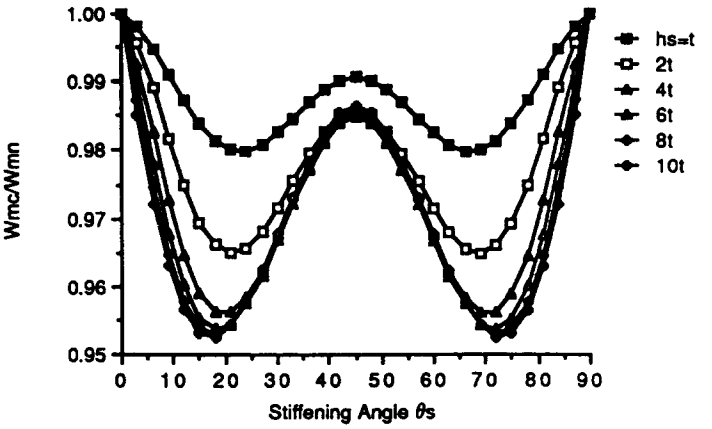

Fig. 4. Joint effects on closed-form solutions of the midpoint deflection for the symmetrically oblique stiffened, rectangular plate with simply-supported edges under the uniform lateral load ($b_s = t$, $d_s = 10t$). The curve shows the midpoint deflection w_{mc} where the joint effects of the stiffeners are taken into account normalized by the value w_{mn} where the joint effects are neglected for the stiffening angle θ_s and the stiffener height h_s.

for various stiffener heights and stiffening angles in both stiffening cases with simply-supported four edges under uniform lateral loads. From Fig. 3, it is observed that in the orthogonal stiffening case, the ratio decreases with increasing h_y/t and it becomes almost constant for h_y/t greater than 5. From this, it can be seen that the midpoint deflection can be reduced when the joint effects of stiffeners are considered for this case. Similarly, in Fig. 4, it can be observed that the ratio decreases with increasing h_s/t and it becomes almost constant for each stiffening angle.

Joint effects on the equivalent rigidities

Figure 5 shows the equivalent bending rigidity D_x, normalized by the bending rigidity of the unstiffened plate D for various stiffener heights in the orthogonal stiffening case.

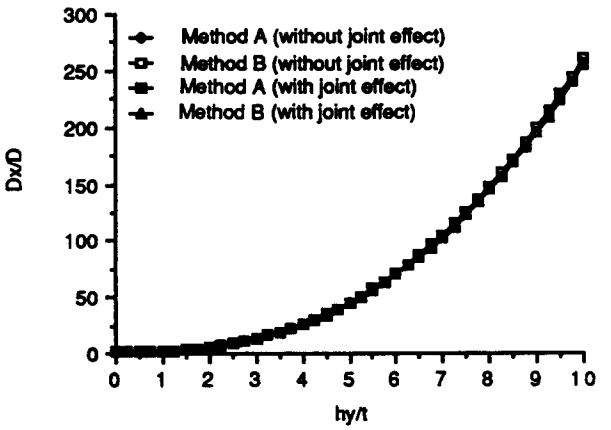

Fig. 5. Joint effects on the equivalent bending rigidity D_x for the orthogonally stiffened, rectangular plate ($b_x = b_y = t$, $h_x = h_y$, $d_x = d_y = 10t$). The curve shows D_x normalized by the bending rigidity D of the unstiffened plate for the stiffener height h_y/t. The solid lines with diamonds and with dotted rectangles represent the results obtained by neglecting the joint effects of stiffeners and by including those values from the concept of the adjusted centroid, respectively, and the solid lines with rectangles and with triangles represent the results obtained by neglecting the joint effects of stiffeners and by including those values from the assumption that the gradient of the in-plane stress resultant is zero, respectively.

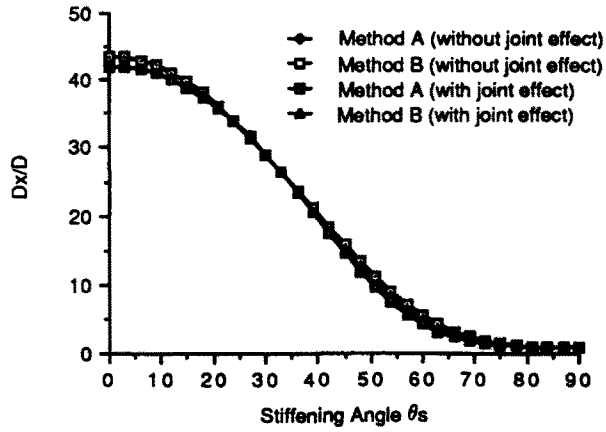

Fig. 6. Joint effects on the equivalent bending rigidity D_x for the symmetrically oblique stiffened, rectangular plate ($b_s = t$, $h_s = 4t$, $d_s = 10t$). The curve shows D_x normalized by the bending rigidity D of the unstiffened plate for the stiffening angle θ_s. The solid lines with diamonds and with dotted rectangles represent the results obtained by neglecting the joint effects of stiffeners and by including those values from the concept of the adjusted centroid, respectively, and the solid lines with rectangles and with triangles represent the results obtained by neglecting the joint effects of stiffeners and by including those values from the assumption that the gradient of the in-plane stress resultant is zero, respectively.

Figures 6 and 7 show D_x for various stiffening angles and stiffener heights, respectively, in the symmetrically oblique stiffening case. In Fig. 5, it can be observed that as the stiffener height increases, the equivalent bending rigidity increases and it is also seen that the rigidities obtained by method A are almost the same as those by B and the joint effects are insignificant. In Figs 6 and 7, it can be observed that the behavior in the case of symmetrically oblique stiffening is similar to that in Fig. 5 for various stiffening angles but the rigidities by method A are a little larger than those by B and the discrepancy increases as the stiffener height increases.

Figure 8 shows the equivalent torsional rigidity D_{xy}, normalized by the torsional rigidity of the unstiffened plate $D_{xy}(iso.)(= Gt^3/6)$ for various stiffener heights in the orthogonal stiffening case, and Figs 9 and 10 show the results for various stiffening angles and

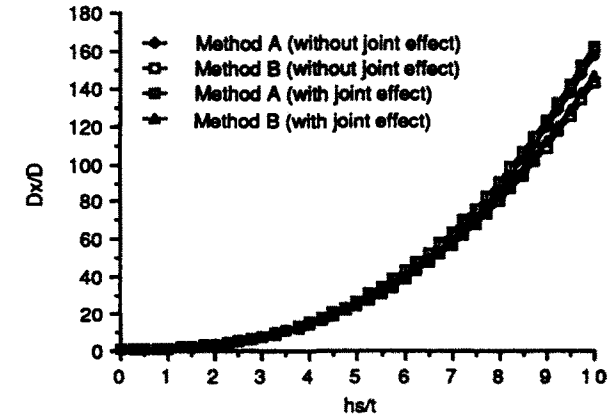

Fig. 7. Joint effects on the equivalent bending rigidity D_x for the symmetrically oblique stiffened, rectangular plate ($b_s = t$, $d_s = 10t$, $\theta_s = 45°$). The curve shows D_x normalized by the bending rigidity D of the unstiffened plate for the stiffener height h_s/t. The solid lines with diamonds and with dotted rectangles represent the results obtained by neglecting the joint effects of stiffeners and by including those values from the concept of the adjusted centroid, respectively, and the solid lines with rectangles and with triangles represent the results obtained by neglecting the joint effects of stiffeners and by including those values from the assumption that the gradient of the in-plane stress resultant is zero, respectively.

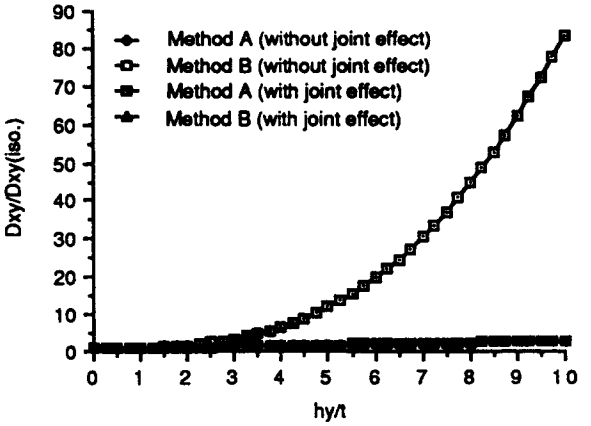

Fig. 8. Joint effects on the torsional rigidity D_{xy} for the orthogonally stiffened, rectangular plate ($b_x = b_y = t$, $h_x = h_y$, $d_x = d_y = 10t$). The curve shows D_{xy} normalized by the torsional rigidity $D_{xy}(iso.)$ of the unstiffened plate for the stiffener height h_y/t. The solid lines with diamonds and with dotted rectangles represent the results obtained by neglecting the joint effects of stiffeners and by including those values from the concept of the adjusted centroid, respectively, and the solid lines with rectangles and with triangles represent the results obtained by neglecting the joint effects of stiffeners and by including those values from the assumption that the gradient of the in-plane stress resultant is zero, respectively.

stiffener heights in the symmetrically oblique stiffening case, respectively. In Fig. 8, it can be seen that as the stiffener height increases, the equivalent torsional rigidity increases and the rigidities by method A are larger than those by B. The torsional rigidities obtained by considering the joint effects are the same as those by neglecting the joint effects. In Figs 9 and 10, it can be seen that the rigidities by method A are larger than those by B and the discrepancy is the largest at the stiffening angle $\theta_s = 45°$. For various stiffening angles and stiffener heights, however, the rigidities obtained by considering the joint effects are a little larger than those by neglecting the joint effects.

Figures 11–13 show the corner deflections of the plate w_c, normalized by the deflections $w_c(iso.)$ of the unstiffened plate at the corner, for various stiffener heights and stiffening

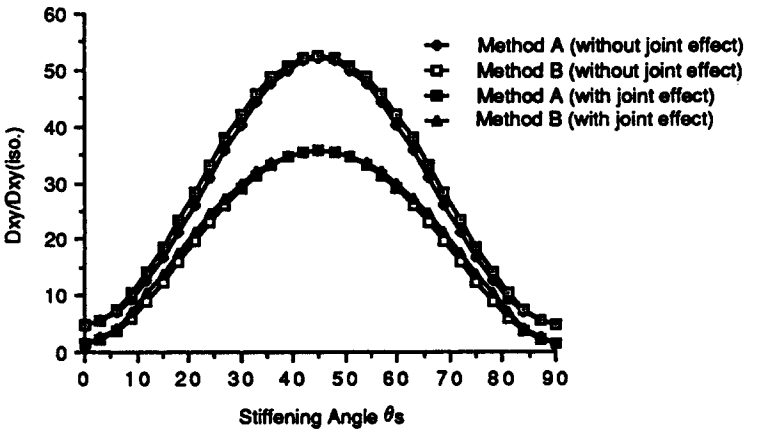

Fig. 9. Joint effects on the equivalent torsional rigidity D_{xy} for the symmetrically oblique stiffened, rectangular plate ($b_s = t$, $h_s = 4t$, $d_s = 10t$). The curve shows D_{xy} normalized by the torsional rigidity $D_{xy}(iso.)$ of the unstiffened plate for the stiffening angle θ_s. The solid lines with diamonds and with dotted rectangles represent the results obtained by neglecting the joint effects of stiffeners and by including those values from the concept of the adjusted centroid, respectively, and the solid lines with rectangles and with triangles represent the results obtained by neglecting the joint effects of stiffeners and by including those values from the assumption that the gradient of the in-plane stress resultant is zero, respectively.

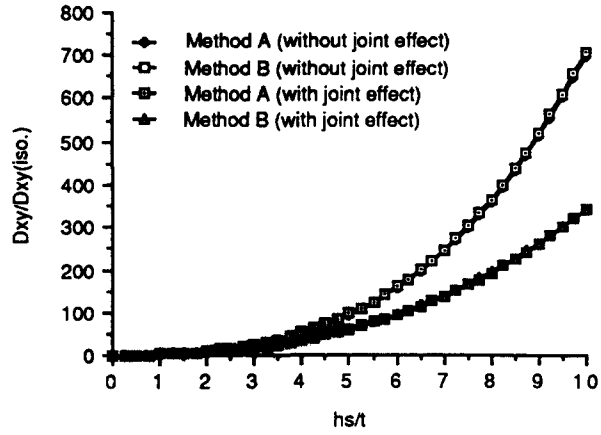

Fig. 10. Joint effects in the equivalent torsional rigidity D_{xy} for the symmetrically oblique stiffened, rectangular plate ($b_s = t$, $d_s = 10t$, $\theta_s = 45°$). The curve shows D_{xy} normalized by the torsional rigidity $D_{xy}(iso.)$ of the unstiffened plate for the stiffener height h_s/t. The solid lines with diamonds and with dotted rectangles represent the results obtained by neglecting the joint effects of stiffeners and by including those values from the concept of the adjusted centroid, respectively, and the solid lines with rectangles and with triangles represent the results obtained by neglecting the joint effects of stiffeners and by including those values from the assumption that the gradient of the in-plane stress resultant is zero, respectively.

angles in both stiffening cases with point-supported three corners under the lateral point load at one corner (pure torsion problem). The results are obtained by using the equivalent torsional rigidity D_{xy}. From Fig. 11 it is observed that the relative deflection decreases with increasing h_y/t for the orthogonal stiffening case. As shown in Fig. 11, the relative deflections obtained by method A are far smaller than those by method B without regard to the joint effects. In Fig. 12, it can be seen that the values by method B are smaller than those by A for various stiffening angles and the discrepancy increases as the stiffening angle θ_s becomes close to 0° and 90°, and that the joint effects are small. In Fig. 13, it can be observed that the relative deflections at the stiffening angle $\theta_s = 45°$ decrease with increasing h_s/t as in Fig. 12.

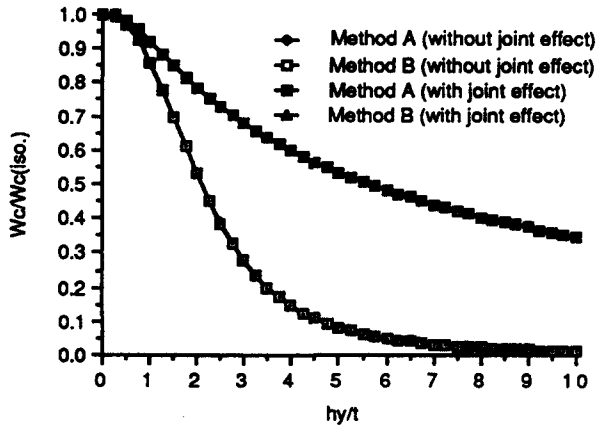

Fig. 11. Joint effects in a pure torsion problem for the orthogonally stiffened, rectangular plate with point-supported corners under the lateral corner load ($b_x = b_y = t$, $h_x = h_y$, $d_x = d_y = 10t$). The curve shows the corner deflection w_c normalized by the value $w_c(iso.)$ of the unstiffened plate for the stiffener height h_s/t. The solid lines with diamonds and with dotted rectangles represent the results obtained by neglecting the joint effects of stiffeners and by including those values from the concept of the adjusted centroid, respectively, and the solid lines with rectangles and with triangles represent the results obtained by neglecting the joint effects of stiffeners and by including those values from the assumption that the gradient of the in-plane stress resultant is zero, respectively.

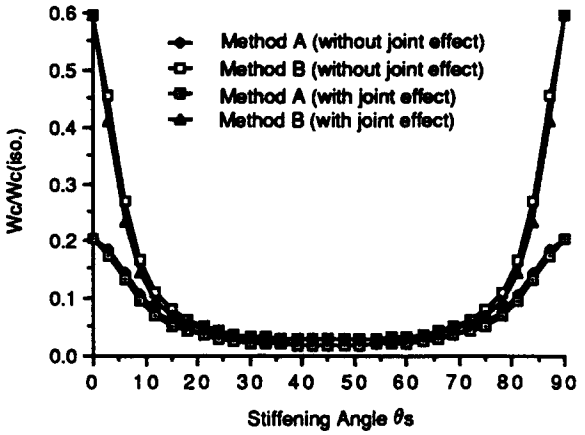

Fig. 12. Joint effects in a pure torsion problem for the symmetrically oblique stiffened, rectangular plate with point-supported corners under the lateral corner load ($b_s = t$, $h_s = 4t$, $d_s = 10t$). The curve shows the corner deflection w_c normalized by the value $w_c(iso.)$ of the unstiffened plate for the stiffening angle θ_s. The solid lines with diamonds and with dotted rectangles represent the results obtained by neglecting the joint effects of stiffeners and by including those values from the concept of the adjusted centroid, respectively, and the solid lines with rectangles and with triangles represent the results obtained by neglecting the joint effects of stiffeners and by including those values from the assumption that the gradient of the in-plane stress resultant is zero, respectively.

Accuracy of the approximate solution

Figures 14–16 show the accuracy of the approximate values $w_m(app.)$ with respect to the accurate values $w_m(acc.)$ for the midpoint deflection in both stiffening cases with simply-supported edges under uniform lateral loads. From Fig. 14 it can be seen that in the orthogonal stiffening case, the values obtained by method B increase a little and those by method A decrease a little with increasing h_y/t regardless of the joint effects. From Fig. 15 it can be observed that the values by method B agree well with the accurate values without considering the joint effects and the discrepancies increase a little as the stiffening angle θ_s becomes close to 0° and 90° but the discrepancies for method A are much larger than those for B. In Fig. 16 it can be seen that the values by method B agree well with the accurate

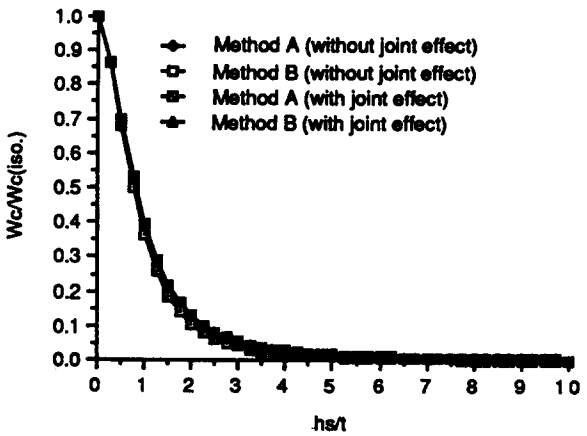

Fig. 13. Joint effects in a pure torsion problem for the symmetrically oblique stiffened, rectangular plate with point-supported corners under the lateral corner load ($b_s = t$, $d_s = 10t$, $\theta_s = 45°$). The curve shows the corner deflection w_c normalized by the value $w_c(iso.)$ of the unstiffened plate for the stiffener height h_s/t. The solid lines with diamonds and with dotted rectangles represent the results obtained by neglecting the joint effects of stiffeners and by including those values from the concept of the adjusted centroid, respectively, and the solid lines with rectangles and with triangles represent the results obtained by neglecting the joint effects of stiffeners and by including those values from the assumption that the gradient of the in-plane stress resultant is zero, respectively.

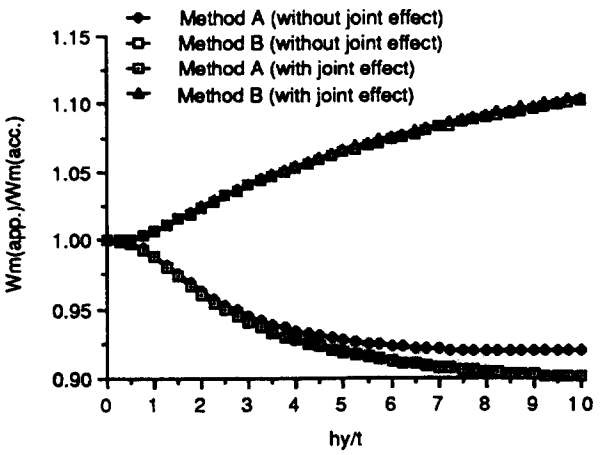

Fig. 14. Accuracy of approximate midpoint deflection $w_m(app.)$ for the orthogonally stiffened, rectangular plate with simply-supported edges under a uniform lateral load ($b_x = b_y = t$, $h_x = h_y$, $d_x = d_y = 10t$). The curve shows $w_m(app.)$ normalized by the accurate value $w_m(acc.)$ for the stiffener height h_y/t. The solid lines with diamonds and with dotted rectangles represent the results obtained by neglecting the joint effects of stiffeners and by including those values from the concept of the adjusted centroid, respectively, and the solid lines with rectangles and with triangles represent the results obtained by neglecting the joint effects of stiffeners and by including those values from the assumption that the gradient of the in-plane stress resultant is zero, respectively.

values but the values by method A decrease considerably for various h_s/t at the stiffening angle $\theta_s = 45°$ without regard to consideration of the joint effects.

5. CONCLUSIONS

In this study the equilibrium equations for stiffened plates with arbitrarily oblique and equally spaced eccentric stiffeners in which the joint effects of the stiffeners are taken into account are derived by applying the principle of minimum potential energy.

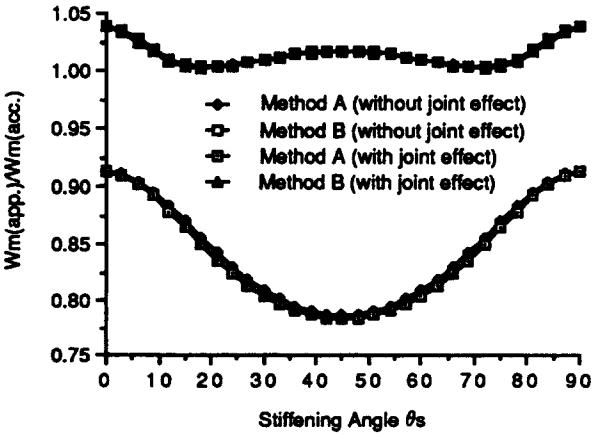

Fig. 15. Accuracy of approximate midpoint deflection $w_m(app.)$ for the symmetrically oblique stiffened, rectangular plate with simply-supported edges under a uniform lateral load ($b_s = t$, $h_s = 4t$, $d_s = 10t$). The curve shows $w_m(app.)$ normalized by the accurate value $w_m(acc.)$ for the stiffening angle θ_s. The solid lines with diamonds and with dotted rectangles represent the results obtained by neglecting the joint effects of stiffeners and by including those values from the concept of the adjusted centroid, respectively, and the solid lines with rectangles and with triangles represent the results obtained by neglecting the joint effects of stiffeners and by including those values from the assumption that the gradient of the in-plane stress resultant is zero, respectively.

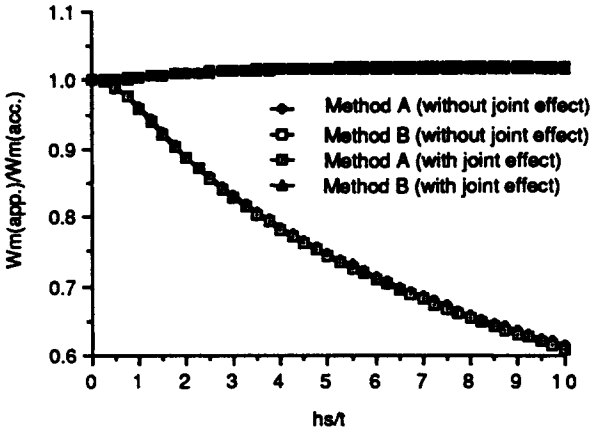

Fig. 16. Accuracy of approximate midpoint deflection $w_m(app.)$ for the symmetrically oblique stiffened, rectangular plate with simply-supported edges under a uniform lateral load ($b_s = t$, $d_s = 10t$, $\theta_s = 45°$). The curve shows $w_m(app.)$ normalized by the accurate value $w_m(acc.)$ for the stiffener height h_s/t. The solid lines with diamonds and with dotted rectangles represent the results obtained by neglecting the joint effects of stiffeners and by including those values from the concept of the adjusted centroid, respectively, and the solid lines with rectangles and with triangles represent the results obtained by neglecting the joint effects of stiffeners and by including those values from the assumption that the gradient of the in-plane stress resultant is zero, respectively.

The closed-form solutions and the approximate solutions by the Huber-type equation for the lateral deflection of the plate are obtained for the orthogonal and symmetrically oblique stiffening cases with simply-supported four edges under uniform lateral loads.

From the numerical results, the joint effects on the closed-form solutions and on the equivalent rigidities and the accuracy of the approximate solutions are summarized as follows.

(1) The lateral deflection of the plate can be reduced a little by considering the joint effects of stiffeners for various stiffener heights in the orthogonal stiffening case and for various stiffening angles in the symmetrically oblique stiffening case with simply-supported four edge under uniform lateral loads.

(2) The joint effects of stiffeners on the equivalent bending rigidity D_x are very small for both stiffening cases and those effects on the equivalent torsional rigidity D_{xy} are also very small for the symmetrically oblique stiffening case.

(3) The D_x obtained by using the concept of adjusted centroids are almost the same as those values obtained by assuming that the gradients of the in-plane stress resultants are zero for both stiffening cases and the D_{xy} obtained by the former method are also almost the same as those obtained by the latter method for the symmetrically oblique stiffening case, but the D_{xy} by the former method are evaluated to be higher than the values by the latter method for the orthogonal stiffening case.

(4) The approximate values of the lateral deflection obtained by the latter method by considering the joint effects of the stiffeners are very close to the accurate values for various stiffener heights and stiffening angles in both stiffening cases.

Acknowledgements—The author wishes to acknowledge the helpful advice of Prof. Charles R. Steele of the Division of Applied Mechanics, Stanford University during this investigation. This work was supported by the Korean Science and Engineering Foundation.

REFERENCES

Argiris, J. H. (1966). Matrix displacement analysis of plates and shells. *Ing. Arch.* **35**, 102–142.

Brush, D. O. and Almroth, B. O. (1975). *Buckling of Bars, Plates, and Shells*. McGraw-Hill, New York.

Clifton, R. J., Chang, J. C. L. and Au, T. (1956). Analysis of orthotropic plate bridges. *J. Struct. Div. ASCE* **89** (ST5), Proc. Paper 3675, 133–171.

Cusens, A. R., Zeiden, M. A. and Pama, R. P. (1972). Elastic rigidity of ribbed plates. *Building Sci.* **7**, 23–32.

Dow, N. F., Libove, C. and Hubka, R. E. (1954). Formulas for the elastic constants of plates with integral waffle-like stiffening. NACA Report 1195.
Flügge, W. (1973). *Stresses in Shells*, second Edn. Springer, New York, Heidelberg, Berlin.
Giencke, E. (1955). Die Grundgleichungen für die orthotrope Platte mit exitentrishen Steifen. *Stahlbau* **24**(6), 128–129.
Hasegawa, A., Akiyama, H. and Nishino, F. (1975). Analysis of plates with single-sided stiffeners. *Trans. JSCE* **270**, 23–34.
Huber, M. T. (1923). Die Theorie der Kreuzweise bewehrten Eisenbeton-Platte, nebst Anwendungen auf mehrere bautechnisch wichtige Aufgaben über rechteckige Platten. *Bauingenieur* **4**, 354–360, 392–395.
Huffington, N. J. Jr. (1956). Theoretical determination of rigidity properties of orthogonally stiffened plates. *J. Appl. Mech.* **23**(1), 15–20.
Karmakar, R. (1979). Buckling of waffle cylinders. *Aeronautical Jl* **83**, 274–278.
Massenet, Ch. (1959). Plaques et coques cylindriques orthotropes a nervures dissymetriques. *Int. Assoc. Bridge Structural Engng* **19**, 201–230.
McElman, J. A., Mikulas, M. M. and Stein, M. (1966). Static and dynamic effects of eccentric stiffening of plates and cylindrical shells. *AIAA Jl* **4**, 887–894.
Meyer, R. R. (1967). Buckling of 45° eccentric-stiffened waffle cylinders. *J. RAeS* **71**, 516–520.
Morley, L. S. D. (1963). *Skew Plates and Structures*. Pergamon Press, Oxford.
Nishino, F., Pama, R. P. and Lee, S. L. (1974). Orthotropic plates with eccentric stiffeners. *Int. Assoc. Bridge Structural Engng* **34-II**, 117–129.
Pflüger, A. (1947). Zum Beulproblem der anisotropen Rechteckplatte. *Ing. Arch.* **16**, 111–120.
Srinivasan, R. S. and Thiruvenkatachari, V. (1985). Static and dynamic analysis of stiffened plates. *Comput. Struct.* **21**(3), 395–403.
Trenks, K. (1954). Beitrag zum Berechnung orthogonal anisotroper Rechteckplatten. *Bauingenieur* **29**(10), 372–377.

APPENDIX

Stiffness coefficients

$$C_{11} = C + Eh_\beta[\eta_\alpha \cos^2\theta_\alpha(A_1\cos^2\theta_\alpha + A_2\cos^2\theta_\beta + 2A_3\cos\theta_\alpha\cos\theta_\beta) + \eta_\beta\cos^2\theta_\beta(B_1\cos^2\theta_\alpha + B_2\cos^2\theta_\beta + 2B_3\cos\theta_\alpha\cos\theta_\beta)]$$

$$C_{12} = \nu C + \frac{Eh_\beta}{2}\left\{\eta_\alpha\left[\frac{A_1}{2}\sin^2 2\theta_\alpha + A_2(\sin^2\theta_\alpha\cos^2\theta_\beta + \cos^2\theta_\alpha\sin^2\theta_\beta) + A_3\sin 2\theta_\alpha\sin(\theta_\alpha+\theta_\beta)\right] + \eta_\beta\left[B_1(\sin^2\theta_\alpha\cos^2\theta_\beta + \cos^2\theta_\alpha\sin^2\theta_\beta) + \frac{B_2}{2}\sin^2 2\theta_\beta + B_3\sin 2\theta_\beta\sin(\theta_\alpha+\theta_\beta)\right]\right\}$$

$$C_{13} = \frac{Eh_\beta}{2}\left\{\eta_\alpha\left\{A_1\cos^2\theta_\alpha\sin 2\theta_\alpha + \frac{A_2}{2}(\cos^2\theta_\alpha\sin 2\theta_\beta + \cos^2\theta_\beta\sin 2\theta_\alpha) + A_3[\cos^2\theta_\alpha\sin(\theta_\alpha+\theta_\beta) + \sin 2\theta_\alpha\cos\theta_\alpha\cos\theta_\beta] - \frac{\xi\csc\phi}{2(1+\nu)}\cos^2\theta_\alpha\sin 2\theta_\beta\right\} + \eta_\beta\left\{\frac{B_1}{2}(\cos^2\theta_\alpha\sin 2\theta_\beta + \cos^2\theta_\beta\sin 2\theta_\alpha) + B_2\cos^2\theta_\beta\sin 2\theta_\beta + B_3[\cos^2\theta_\beta\sin(\theta_\alpha+\theta_\beta) + \sin 2\theta_\beta\cos\theta_\alpha\cos\theta_\beta] - \frac{\xi\csc\phi}{2(1+\nu)}\cos^2\theta_\beta\sin 2\theta_\alpha\right\}\right\}$$

$$C_{14} = e_\beta Eh_\beta[\eta_\alpha\cos^2\theta_\alpha(A_1\cos^2\theta_\alpha + A_2\cos^2\theta_\beta + 2A_3\cos\theta_\alpha\cos\theta_\beta) + \eta_\beta\cos^2\theta_\beta(B_1\cos^2\theta_\alpha + B_2\cos^2\theta_\beta + 2B_3\cos\theta_\alpha\cos\theta_\beta)]$$

$$C_{15} = \frac{e_\beta Eh_\beta}{2}\left\{\eta_\alpha\left[\frac{A_1}{2}\sin^2 2\theta_\alpha + A_2(\sin^2\theta_\alpha\cos^2\theta_\beta + \cos^2\theta_\alpha\sin^2\theta_\beta) + A_3\sin 2\theta_\alpha\sin(\theta_\alpha+\theta_\beta)\right] + \eta_\beta\left[B_1(\sin^2\theta_\alpha\cos^2\theta_\beta + \cos^2\theta_\alpha\sin^2\theta_\beta) + \frac{B_2}{2}\sin^2 2\theta_\beta + B_3\sin 2\theta_\beta\sin(\theta_\alpha+\theta_\beta)\right]\right\}$$

$$C_{16} = 2e_\beta C_{13}$$

$$C_{22} = C + Eh_\beta[\eta_\alpha\sin^2\theta_\alpha(A_1\sin^2\theta_\alpha + A_2\sin^2\theta_\beta + 2A_3\sin\theta_\alpha\sin\theta_\beta) + \eta_\beta\sin^2\theta_\beta(B_1\sin^2\theta_\alpha + B_2\sin^2\theta_\beta + 2B_3\sin\theta_\alpha\sin\theta_\beta)]$$

$$C_{23} = \frac{Eh_\beta}{2}\left\{\eta_\alpha\left\{A_1 \sin^2\theta_\alpha \sin 2\theta_\alpha + \frac{A_2}{2}(\sin^2\theta_\alpha \sin 2\theta_\beta + \sin^2\theta_\beta \sin 2\theta_\alpha)\right.\right.$$
$$\left. + A_3[\sin^2\theta_\alpha \sin(\theta_\alpha+\theta_\beta) + \sin 2\theta_\alpha \sin\theta_\alpha \sin\theta_\beta] - \frac{\xi \csc\phi}{2(1+\nu)} \sin^2\theta_\alpha \sin 2\theta_\beta\right\}$$
$$+\eta_\beta\left[\frac{B_1}{2}(\sin^2\theta_\alpha \sin 2\theta_\beta + \sin^2\theta_\beta \sin 2\theta_\alpha) + B_2 \sin^2\theta_\beta \sin 2\theta_\beta\right.$$
$$\left.\left. + B_3[\sin^2\theta_\beta \sin(\theta_\alpha+\theta_\beta) + \sin 2\theta_\beta \sin\theta_\alpha \sin\theta_\beta] - \frac{\xi \csc\phi}{2(1+\nu)} \sin^2\theta_\beta \sin 2\theta_\alpha\right]\right\}$$

$$C_{24} = C_{15}$$

$$C_{25} = e_\beta Eh_\beta[\eta_\alpha \sin^2\theta_\alpha(A_1 \sin^2\theta_\alpha + A_2 \sin^2\theta_\beta + 2A_3 \sin\theta_\alpha \sin\theta_\beta)$$
$$+\eta_\beta \sin^2\theta_\beta(B_1 \sin^2\theta_\alpha + B_2 \sin^2\theta_\beta + 2B_3 \sin\theta_\alpha \sin\theta_\beta)]$$

$$C_{26} = 2e_\beta C_{23}$$

$$C_{33} = \frac{1-\nu}{2}C + \frac{Eh_\beta}{4}\left\{\eta_\alpha\left[A_1 \sin^2 2\theta_\alpha + A_2 \sin 2\theta_\alpha \sin 2\theta_\beta\right.\right.$$
$$\left. + 2A_3 \sin 2\theta_\alpha \sin(\theta_\alpha+\theta_\beta) - \frac{\xi \csc\phi}{1+\nu} \sin 2\theta_\alpha \sin 2\theta_\beta\right]$$
$$+\eta_\beta\left[B_1 \sin 2\theta_\alpha \sin 2\theta_\beta + B_2 \sin^2 2\theta_\beta\right.$$
$$\left.\left. + 2B_3 \sin 2\theta_\beta \sin(\theta_\alpha+\theta_\beta) - \frac{\xi \csc\phi}{1+\nu} \sin 2\theta_\alpha \sin 2\theta_\beta\right]\right\}$$

$$C_{34} = e_\beta C_{13}$$

$$C_{35} = e_\beta C_{23}$$

$$C_{36} = \frac{e_\beta Eh_\beta}{2}\left\{\eta_\alpha\left[A_1 \sin^2 2\theta_\alpha + A_2 \sin 2\theta_\alpha \sin 2\theta_\beta\right.\right.$$
$$\left. + 2A_3 \sin 2\theta_\alpha \sin(\theta_\alpha+\theta_\beta) - \frac{\xi \csc\phi}{1+\nu} \sin 2\theta_\alpha \sin 2\theta_\beta\right]$$
$$+\eta_\beta\left[B_1 \sin 2\theta_\alpha \sin 2\theta_\beta + B_2 \sin^2 2\theta_\beta\right.$$
$$\left.\left. + 2B_3 \sin 2\theta_\beta \sin(\theta_\alpha+\theta_\beta) - \frac{\xi \csc\phi}{1+\nu} \sin 2\theta_\alpha \sin 2\theta_\beta\right]\right\}$$

$$C_{44} = D + E\left[\frac{I_\alpha}{d_\alpha}\cos^2\theta_\alpha(A_1 \cos^2\theta_\alpha + A_2 \cos^2\theta_\beta + 2A_3 \cos\theta_\alpha \cos\theta_\beta)\right.$$
$$\left. + \frac{I_\beta}{d_\beta}\cos^2\theta_\beta(B_1 \cos^2\theta_\alpha + B_2 \cos^2\theta_\beta + 2B_3 \cos\theta_\alpha \cos\theta_\beta)\right]$$
$$+ \frac{G}{4}\left(\frac{J_\alpha}{d_\alpha}\sin^2 2\theta_\alpha + \frac{J_\beta}{d_\beta}\sin^2 2\theta_\beta\right)$$

$$C_{45} = \nu D + \frac{E}{2}\left\{\frac{I_\alpha}{d_\alpha}\left[\frac{A_1}{2}\sin^2 2\theta_\alpha + A_2(\sin^2\theta_\alpha \cos^2\theta_\beta\right.\right.$$
$$\left. + \cos^2\theta_\alpha \sin^2\theta_\beta) + A_3 \sin 2\theta_\alpha \sin(\theta_\alpha+\theta_\beta)\right]$$
$$+ \frac{I_\beta}{d_\beta}\left[B_1(\sin^2\theta_\alpha \cos^2\theta_\beta + \cos^2\theta_\alpha \sin^2\theta_\beta)\right.$$
$$\left.\left. + \frac{B_2}{2}\sin^2 2\theta_\beta + B_3 \sin 2\theta_\beta \sin(\theta_\alpha+\theta_\beta)\right]\right\} - \frac{G}{4}\left(\frac{J_\alpha}{d_\alpha}\sin^2 2\theta_\alpha + \frac{J_\beta}{d_\beta}\sin^2 2\theta_\beta\right)$$

$$C_{46} = E\left\{\frac{I_\alpha}{d_\alpha}\left\{A_1 \cos^2\theta_\alpha \sin 2\theta_\alpha + \frac{A_2}{2}(\cos^2\theta_\alpha \sin 2\theta_\beta + \cos^2\theta_\beta \sin 2\theta_\alpha)\right.\right.$$
$$\left.\left. + A_3[\cos^2\theta_\alpha \sin(\theta_\alpha+\theta_\beta) + \sin 2\theta_\alpha \cos\theta_\alpha \cos\theta_\beta] - \frac{\xi \csc\phi}{2(1+\nu)} \cos^2\theta_\alpha \sin 2\theta_\beta\right\}\right.$$

$$+\frac{I_\beta}{d_\beta}\left\{\frac{B_1}{2}(\cos^2\theta_x\sin 2\theta_\beta+\cos^2\theta_\beta\sin 2\theta_x)+B_2\cos^2\theta_\beta\sin 2\theta_\beta\right.$$

$$\left.+B_3[\cos^2\theta_\beta\sin(\theta_x+\theta_\beta)+\sin 2\theta_\beta\cos\theta_x\cos\theta_\beta]-\frac{\xi\csc\phi}{2(1+\nu)}\cos^2\theta_\beta\sin 2\theta_x\right\}\Bigg\}$$

$$-\frac{G}{4}\left(\frac{J_x}{d_x}\sin 4\theta_x-\frac{J_\beta}{d_\beta}\sin 4\theta_\beta\right)$$

$$C_{55}=D+E\left[\frac{I_x}{d_x}\sin^2\theta_x(A_1\sin^2\theta_x+A_2\sin^2\theta_\beta+2A_3\sin\theta_x\sin\theta_\beta)\right.$$

$$\left.+\frac{I_\beta}{d_\beta}\sin^2\theta_\beta(B_1\sin^2\theta_x+B_2\sin^2\theta_\beta+2B_3\sin\theta_x\sin\theta_\beta)\right]$$

$$+\frac{G}{4}\left(\frac{J_x}{d_x}\sin^2 2\theta_x+\frac{J_\beta}{d_\beta}\sin^2 2\theta_\beta\right)$$

$$C_{56}=E\left\{\frac{I_x}{d_x}\left\{A_1\sin^2\theta_x\sin 2\theta_x+\frac{A_2}{2}(\sin^2\theta_x\sin 2\theta_\beta+\sin^2\theta_\beta\sin 2\theta_x)\right.\right.$$

$$\left.+A_3[\sin^2\theta_x\sin(\theta_x+\theta_\beta)+\sin 2\theta_x\sin\theta_x\sin\theta_\beta]-\frac{\xi\csc\phi}{2(1+\nu)}\sin^2\theta_x\sin 2\theta_\beta\right\}$$

$$+\frac{I_\beta}{d_\beta}\left\{\frac{B_1}{2}(\sin^2\theta_x\sin 2\theta_\beta+\sin^2\theta_\beta\sin 2\theta_x)+B_2\sin^2\theta_\beta\sin 2\theta_\beta\right.$$

$$\left.\left.+B_3[\sin^2\theta_\beta\sin(\theta_x+\theta_\beta)+\sin 2\theta_\beta\sin\theta_x\sin\theta_\beta]-\frac{\xi\csc\phi}{2(1+\nu)}\sin^2\theta_\beta\sin 2\theta_x\right\}\right\}$$

$$+\frac{G}{4}\left(\frac{J_x}{d_x}\sin 4\theta_x-\frac{J_\beta}{d_\beta}\sin 4\theta_\beta\right)$$

$$C_{66}=2(1-\nu)D+E\left\{\frac{I_x}{d_x}\left[A_1\sin^2 2\theta_x+A_2\sin 2\theta_x\sin 2\theta_\beta\right.\right.$$

$$\left.+2A_3\sin 2\theta_x\sin(\theta_x+\theta_\beta)-\frac{\xi\csc\phi}{1+\nu}\sin 2\theta_x\sin 2\theta_\beta\right]$$

$$+\frac{I_\beta}{d_\beta}\left[B_1\sin 2\theta_x\sin 2\theta_\beta+B_2\sin^2 2\theta_\beta\right.$$

$$\left.\left.+2B_3\sin 2\theta_\beta\sin(\theta_x+\theta_\beta)-\frac{\xi\csc\phi}{1+\nu}\sin 2\theta_x\sin 2\theta_\beta\right]\right\}$$

$$+G\left(\frac{J_x}{d_x}\cos^2 2\theta_x+\frac{J_\beta}{d_\beta}\cos^2 2\theta_\beta\right)$$

$$C_{ij}=C_{ji} \tag{A1}$$

where

$$e_\beta=\frac{t+h_\beta}{2}$$

$$I_x=\frac{b_x h_\beta^3}{12}+e_\beta^2 b_x h_\beta$$

$$I_\beta=\frac{b_\beta h_\beta^3}{12}+e_\beta^2 b_\beta h_\beta$$

$$J_x=Kb_x^3 h_\beta$$

$$J_\beta=Kb_\beta^3 h_\beta. \tag{A2}$$

Boundary conditions

The boundary conditions to be satisfied at $x=0$ and a are

$$[C_{41}u_{,x}+C_{42}v_{,y}+C_{43}(u_{,y}+v_{,x})-C_{44}w_{,xx}-C_{45}w_{,yy}-C_{46}w_{,xy}]_{,x}+[C_{61}u_{,x}+C_{62}v_{,y}+C_{63}(u_{,y}+v_{,x})$$
$$-C_{64}w_{,xx}-C_{65}w_{,yy}-C_{66}w_{,xy}]_{,y}=0 \quad \text{or} \quad w=0$$

$$C_{41}u_{,x}+C_{42}v_{,y}+C_{43}(u_{,y}+v_{,x})-C_{44}w_{,xx}-C_{45}w_{,yy}-C_{46}w_{,xy}=0 \quad \text{or} \quad w_{,x}=0$$

$$[C_{11}u_{,x}+C_{12}v_{,y}+C_{13}(u_{,y}+v_{,x})-C_{14}w_{,xx}-C_{15}w_{,yy}-C_{16}w_{,xy}]_{,y}=0 \quad \text{or} \quad u=0$$

$$C_{31}u_{,x}+C_{32}v_{,y}+C_{33}(u_{,y}+v_{,x})-C_{34}w_{,xx}-C_{35}w_{,yy}-C_{36}w_{,xy}=0 \quad \text{or} \quad v=0 \tag{A3}$$

and those at $y=0$ and b are

$$\begin{aligned}
&[C_{51}u_{,x}+C_{52}v_{,y}+C_{53}(u_{,y}+v_{,x})-C_{54}w_{,xx}-C_{55}w_{,yy}-C_{56}w_{,xy}]_{,y}+[C_{51}u_{,x}+C_{52}v_{,y}+C_{53}(u_{,y}+v_{,x})\\
&\qquad -C_{54}w_{,xx}-C_{55}w_{,yy}-C_{56}w_{,xy}]_{,x}=0 \quad \text{or} \quad w=0\\
&C_{51}u_{,x}+C_{52}v_{,y}+C_{53}(u_{,y}+v_{,x})-C_{54}w_{,xx}-C_{55}w_{,yy}-C_{56}w_{,xy}=0 \quad \text{or} \quad w_{,y}=0\\
&[C_{21}u_{,x}+C_{22}v_{,y}+C_{23}(u_{,y}+v_{,x})-C_{24}w_{,xx}-C_{25}w_{,yy}-C_{26}w_{,xy}]_{,y}=0 \quad \text{or} \quad v=0\\
&C_{31}u_{,x}+C_{32}v_{,y}+C_{33}(u_{,y}+v_{,x})-C_{34}w_{,xx}-C_{35}w_{,yy}-C_{36}w_{,xy}=0 \quad \text{or} \quad u=0.
\end{aligned} \tag{A4}$$

Equivalent rigidities

From eqn (A1), equivalent bending and torsional rigidities obtained on the assumption that the normal strain is zero at the adjusted centroid of the cross-section in each direction can be represented as follows:

$$\begin{aligned}
D_x &= C_{44}-C_{14}\bar{e}_x\\
H &= C_{45}+C_{12}\bar{e}_x\bar{e}_y+\tfrac{1}{2}[C_{66}+C_{33}(\bar{e}_x+\bar{e}_y)^2]\\
D_y &= C_{55}-C_{25}\bar{e}_y
\end{aligned} \tag{A5}$$

where

$$\begin{aligned}
\bar{e}_x &= \frac{C_{14}}{C_{11}}\\
\bar{e}_y &= \frac{C_{25}}{C_{22}}.
\end{aligned} \tag{A6}$$